

High-echoic line tracing of transthoracic echocardiography accurately assesses right ventricular enlargement in adult patients with atrial septal defect

佐藤, 翼

<https://hdl.handle.net/2324/6787493>

出版情報 : Kyushu University, 2022, 博士 (保健学), 課程博士

バージョン :

権利関係 : Public access to the fulltext file is restricted for unavoidable reason (2)



**High-echoic Line Tracing of Transthoracic Echocardiography
Accurately Assesses Right Ventricular Enlargement in Adult Patients
with Atrial Septal Defect**

Tasuku Sato, RMS^{1,2)}, Ichiro Sakamoto, MD³⁾, Ken-ichi Hiasa, MD, PhD³⁾, Masateru
Kawakubo, PhD⁴⁾, Ayako Ishikita, MD, PhD³⁾, Shintaro Umemoto, MD, PhD³⁾, Min-
Jeong Kang, PhD¹⁾, Hiroyuki Sawatari, PhD⁵⁾, Akiko Chishaki, MD, PhD⁶⁾, Hiroshi
Shigeto, MD, PhD⁴⁾, Hiroyuki Tsutsui, MD, PhD³⁾

¹⁾ Department of Health Sciences, Graduate School of Medical Sciences, Kyushu
University, Fukuoka, Japan

²⁾ Heart Center, Kyushu University Hospital, Fukuoka, Japan

³⁾ Department of Cardiovascular Medicine, Kyushu University Graduate School of
Medical Sciences, Kyushu University, Fukuoka, Japan

⁴⁾ Department of Health Sciences, Faculty of Medical Sciences, Kyushu University,
Fukuoka, Japan

⁵⁾ Department of Health Care for Adults, Graduate School of Biomedical and Health
Sciences, Hiroshima University, Hiroshima, Japan

⁶⁾ Health Care Center, Fukuoka Dental College Hospital, Fukuoka, Japan

20

21 **Short title:** High-echoic tracing of the right ventricle

22

23 **Competing Interests**

24 Tasuku Sato, Ichiro Sakamoto, Masateru Kawakubo, Ayako Ishikita, Shintaro

25 Umemoto, Min-Jeong Kang, Hiroyuki Sawatari, Akiko Chishaki, and Hiroshi Shigeto,

26 declare that there are no conflicts of interest.

27 Ken-ichi Hiasa received remuneration from Daiichi Sankyo, Nippon Boehringer

28 Ingelheim, Pfizer, Bristol-Myers Squibb, Bayer, and Otsuka Pharmaceutical.

29 Hiroyuki Tsutusi received remuneration from Kowa, Teijin Pharma, Nippon Boehringer,

30 Ingelheim, Mitsubishi Tanabe Pharma, Pfizer Japan, Ono Pharmaceutical, Daiichi

31 Sankyo, Novartis Pharma, Bayer Yakuhin, Otsuka Pharmaceutical, and AstraZeneca;

32 manuscript fees from Nippon Rinsho; research funding from Abbott Medical Japan,

33 Otsuka Pharmaceutical, Boston Scientific Japan, Ono Pharmaceutical, Bayer Yakuhin,

34 Nippon Boehringer Ingelheim, St.Mary's Hospital, Teijin Pharma, Daiichi Sankyo, and

35 Mitsubishi Tanabe Pharma; and donations Abbott Medical Japan, Otsuka

36 Pharmaceutical, Boston Scientific Japan, Ono Pharmaceutical, Bayer Yakuhin, Nippon

37 Boehringer Ingelheim, St.Mary's Hospital, Teijin Pharma, Daiichi Sankyo, and

38 Mitsubishi Tanabe Pharma.

39 Hiroyuki Tsutsui is a member of Circulation Journal's editorial team.

40

41 **IRB information**

42 The study protocol was approved by the Ethics Committee of Kyushu University

43 Hospital (Approval number: 2020-39), and the study complied with the 1964

44 Declaration of Helsinki and its later amendments.

45

46 Kyusyu University (Tasuku Sato, Ichiro Sakamoto, Ken-ichi Hiasa, Ayako Ishikita,

47 Shintaro Umemoto, Min-Jeong Kang, and Hiroyuki Tsutsui), Fukuoka, Japan; Kyushu

48 University Graduate School of Medical Sciences (Masateru Kawakubo and Hiroshi

49 Shigeto), Fukuoka, Japan; Hiroshima University (Hiroyuki Sawatari), Hiroshima,

50 Japan; Fukuoka Dental College Hospital (Akiko Chishaki), Fukuoka, Japan

51

52 **Corresponding author**

53 Tasuku Sato, ([Registered Medical Sonographer : RMS](#))

54 Department of Health Sciences, Graduate School of Medical Sciences, Kyushu

55 University, 3-1-1 Maidashi, Higashi-ku, Fukuoka, Japan

56 Tel: +81-92-642-5365

57 Fax: +81-92-642-5374

58 E-mail: sato.tasuku.553@m.kyushu-u.ac.jp

59 **Acknowledgments**

60 This study was supported by a “medical stuff research grant” from the Japanese

61 Circulation Society.

62 We acknowledge the support of the staff of the Heart Center of Kyushu University

63 Hospital (Fukuoka, Japan), especially to Goro Kawahara, Tokiko Koya, Asami Hanada,

64 Yuya Fukudome, Ryoko Hayashi, Miki Kawamura, Manami Ito, and Takuto Moriyama,

65 who acquired the TTE images and data.

66 We would like to thank Editage (www.editage.com) for English language editing.

67

68

Abstract

Purpose: Accurate measurement of right ventricular (RV) size using transthoracic echocardiography (TTE) is important for evaluating the severity of congenital heart diseases. The RV end-diastolic area index (RVEDA_i) determined using TTE is used to assess RV dilatation; however, the tracing line of the RVEDA_i has not been clearly defined by the guidelines. This study aimed to determine the exact tracing method for RVEDA_i using TTE.

Methods: We retrospectively studied 107 patients with atrial septal defects who underwent cardiac magnetic resonance imaging (CMR) and TTE. We measured the RVEDA_i according to isoechoic and high-echoic lines, and compared it with the RVEDA_i measured using CMR. The isoechoic line was defined as the isoechoic endocardial border of the RV free wall, whereas the high-echoic line was defined as the high-echoic endocardial border of the RV free wall more outside than the isoechoic line.

Results: RVEDA_i measured using high-echoic line (high-RVEDA_i) was more accurately related to RVEDA_i measured using CMR than that measured using isoechoic line (iso-RVEDA_i). The difference in the high-RVEDA_i was 0.3 cm²/m², and the limit of agreement (LOA) was −3.7 to 4.3 cm²/m². With regard to inter-observer variability, high-RVEDA_i was superior to iso-RVEDA_i.

87 **Conclusion:** High-RVEDAi had greater agreement with CMR-RVEDAi than with iso-
88 RVEDAi. High-RVEDAi can become the standard measurement of RV size using two-
89 dimensional TTE.

90

91 **Key Words:** Right ventricular end-diastolic area index; Transthoracic
92 echocardiography; Cardiac magnetic resonance imaging; Atrial septal defect

93

94

Introduction

Evaluating right ventricular (RV) size plays a key role in determining the treatment of congenital heart disease. In particular, the 2018 AHA/ACC guidelines for the management of adults with congenital heart disease recommend atrial septal defect (ASD) closure in patients with RV volume overload, regardless of symptoms [1]. However, the appropriate imaging modalities and threshold for RV enlargement remain unclear.

Cardiac magnetic resonance (CMR) is the gold standard for RV measurement, but its high cost limits its frequent use. Conversely, transthoracic echocardiography (TTE) costs less but tends to underestimate RV volume, even when using three-dimensional (3D) TTE [2-7].

Among the many variables measured using two-dimensional (2D) TTE, the right ventricular end-diastolic area index (RVEDAi) is promising because of its good correlation with the right ventricular end-diastolic volume index (RVEDVi) measured using CMR [8-13]. However, line tracing for RVEDAi is not strictly defined. Some reports traced the intima surface of the RV (isoechoic line tracing), whereas others traced more outside (high-echoic line tracing) [12-16]. This causes the RVEDAi tracing line to vary for each sonographer. Thus, in the present study, we aimed to determine the exact tracing method for RVEDAi using TTE.

書式を変更: スペルチェックと文章校正を行う 上付き下付き (なし)

書式を変更: スペルチェックと文章校正を行う 上付き下付き (なし)

書式を変更: フォント: (英) Times New Roman, (日) Times New Roman

書式を変更: スペルチェックと文章校正を行う 上付き下付き (なし)

書式を変更: スペルチェックと文章校正を行う 上付き下付き (なし)

Methods

Study population

We retrospectively investigated the data of patients with ASD who had been assessed for RV volume using CMR and TTE. We excluded patients with 1) an interval between TTE and CMR studies longer than 180 days, and 2) low-quality TTE images, defined as unavailability of the whole RV image, and blurry border between the tissue and the cavity. In the “after transcatheter closure” patients
, consideration of RV remodeling due to hemodynamics
was required. According to previous studies [17, 18], significant RV size
regression was observed within 6 months following transcatheter
closure. Therefore, we included “after transcatheter closure” ASD patients
at 1-year follow-up. The following data were collected from medical records: age, sex, New York Heart Association functional class, TTE, and CMR data.

The study protocol was approved by the Ethics Committee of Kyushu University Hospital (approval number: 2020-39), and the study complied with the principles of the Declaration of Helsinki. Informed consent was obtained in the form of opt-out on the website.

書式を変更: スペルチェックと文章校正を行う 上付き下付き (なし)

134 **CMR**

135 CMR studies were performed using a 3.0-T clinical scanner (Achieva 3.0T TX;
136 Philips Medical Systems, Best, the Netherlands) equipped with a 32-element cardiac
137 coil. Cine steady-state free precession images were obtained with electrocardiographic
138 gating while the patients held their breath for approximately 10–20 s.

139 RVEDV and RVEDA were evaluated using commercial software (IntelliSpace
140 Portal; Philips Healthcare). All RVEDV measurements were performed by axial slices.
141 In the software, RV endocardial borders were contoured with myocardial trabeculations,
142 moderator band, and papillary muscles included in the cavity, as previously reported
143 [19, 20]. RVEDA was gauged in the long-axis four-chamber images at the level of the
144 largest RV dimension in the short-axis view [21] (Figure 1). Based on a previous
145 report, we described RV dilatation as RVEDVi measured using CMR (CMR-RVEDVi)
146 of $>107.5 \text{ mL/m}^2$ and a normal RV as a CMR-RVEDVi of $\leq 107.5 \text{ mL/m}^2$ [22].

147

148 **TTE**

149 All images were acquired by experienced cardiac sonographers using the
150 following ultrasound imaging devices: an EPIQ7G echocardiographic system with an
151 X5-1 transducer (Philips Medical Systems, Andover, MA, USA), an iE33
152 echocardiographic system with an S5-1 transducer (Philips Medical Systems), and a

書式を変更: スペルチェックと文章校正を行う 上付き下付き
(なし)

書式を変更: スペルチェックと文章校正を行う 上付き下付き
(なし)

書式を変更: スペルチェックと文章校正を行う 上付き下付き
(なし)

Vivid95 echocardiographic system with an M5Sc transducer (GE Vingmed Ultrasound AS, Horten, Norway). Echocardiographic images were analyzed using commercial software, such as IntelliSpace Cardiovascular (Philips Ultrasound) and EchoPAC (GE Vingmed Ultrasound AS). The RV was measured in RV-maximized views. We adopted the RV-focused view, obtaining the image with the LV apex at the center of the scanning sector, displaying the largest basal RV diameter, and avoiding the five-chamber view [standard-apical four-chamber views to maximize the RV and clearly identify the RV free wall-23-25]. If it was difficult to visualize the entire RV using the typical RV-focused view, we used a four4-chamber view adjusted so that the RV was visualized to the maximum (RV-maximized view). This view maximized the entire RV, clearly identified the free wall of the RV, and avoided the five5-chambers, although the LV apex could not be centered in the scan sector due to the expansion of the RV (Figure 2a).

The RV free wall was traced in two ways. First, the borderline between the isoechoic area and the cavity was traced, described as the “iso-echoic line tracing” method (Figure 2b). The iso-echo region was defined as the region with the same brightness as the left ventricular (LV) wall, and the echo free area was defined as the region with the same brightness as the heart chamber. As for the RV basal, we marked the apparent border between the isoechoic area and the echo-free area with dots,

書式を変更: スペルチェックと文章校正を行う 上付き下付き (なし)

followed by drawing a line. The protrusions (papillary muscles, moderator band, and trabeculations) may be included in the cavity to adjust the unsmooth borderline. In the RV apical, the line was continuously demarcated from the RV basal, and the intersection of the free wall and septum was sharply traced. The RVEDAi measured ~~in~~by this approach was defined as the “iso-RVEDAi.” Second, the outer border between the high-echoic area and the cavity was traced, described as the “high-echoic line tracing” method (Figure 2c). The high-echoic area was defined as the region with the same brightness as the pericardium. As mentioned above, in the RV basal, we marked the boundaries between the visible high-echoic area with dots and connected them. In the RV apical, the junctions of the trabeculations and edges of the high-echoic line were carefully connected. The intersection of the high-echoic line of the free and septal walls was sharply traced. The RVEDAi measured using the high-echoic line tracing method was described as the “high-RVEDAi.”

The other parts of the RV were gauged according to the American Society of Echocardiography (ASE) guidelines [23-25]. The RV endocardial border was traced from the free wall annulus to the medial annulus via the apex at the end-diastolic phase. The trabeculations, papillary muscles, and moderator band were included in the cavity. For interventricular septum tracing, the border between the cavity and tissue was traced at the recessed portion on the muscle tissue side of the irregular line. The bulges on the

書式を変更: スペルチェックと文章校正を行う 上付き下付き (なし)

cavity side were not traced as part of the trabeculations, moderator band, or papillary muscles.

Inter- and intra-observer variability

The RVEDAi measurements obtained using TTE were tested for inter- and intra-observer variability by one observer for 20 randomly selected patients. The inter-observer variability of the iso-RVEDAi and high-RVEDAi was evaluated by six sonographers with more than three years of experience in echocardiography. The intra-observer variability of the high-RVEDAi was performed by one sonographer at least a month later.

Statistical analysis

Data are shown as median (interquartile range) or number (percentage). Agreement was evaluated using Bland–Altman analysis. The Shapiro-Wilk test was performed for confirming normal or non-normal distribution to evaluate normality, and Spearman's rank correlation coefficient (ρ) was used to investigate the correlation between TTE and CMR measurements. The inter- and intra-observer variabilities of the iso-RVEDAi and high-RVEDAi were evaluated using the coefficient of variability and intraclass correlation coefficient (ICC) with one- or two-way random single measures

(ICC (1,1) or ICC (2,1)). ICCs were defined as excellent ($ICC \geq 0.75$), good ($ICC = 0.60-0.74$), moderate ($ICC = 0.40-0.59$), and poor ($ICC \leq 0.39$). The diagnostic accuracy (sensitivity, specificity, positive predictive value, negative predictive value, and accuracy) and cut-off values were calculated based on the receiver operating characteristic curve. Statistical significance was set at a P-value of <0.05 . All statistical analyses were performed using the JMP software program, version 15 (SAS Institute Inc., Cary, NC, USA).

Results

Patient characteristics

A total of 107 patients were enrolled in this study and 174 examinations were conducted. A total of 64 patients were excluded due to low quality imaging, and three patients were excluded due to having an interval of over 180 days between TTE and CMR. Fifty-seven patients underwent TTE and CMR before transcatheter closure of ASD, and the remaining 50 patients underwent these techniques after the procedure. Of the 57 "before closure" cases of before-closure (53% of all), a short interval of between TTE and CMR (within 7 days) patients were in was associated with 31 cases (54%), an 8-60 day interval patients were with 7 cases (12%), a 61-90 day interval patients were with 7 cases (12%), and a 91-180 day interval patients were with 12 cases (21%).

~~Of the 50 cases of after closure. Of the 50 “after closure” cases of after closure (47% of~~
all), TTE and CMR were performed on the same day in 47 cases (94%), and only three
cases (6%) had TTE and CMR performed within 60 days. Thirty-six patients underwent
TTE and CMR both before and after transcatheter ASD closure. The median age was 59
(interquartile range 44–67) years, and 28 of the patients were men (26%). One hundred
and three patients (96%) had sinus rhythm when TTE and CMR were performed. All
patients had New York Heart Association functional class I or II (Table 1). No adverse
events, such as heart failure or atrial arrhythmias, occurred in any of the subjects.

The TTE data are shown in Table 2. The RV-maximized view was used in 90
cases (84%). The median iso-RVEDAi [$15 \text{ cm}^2/\text{m}^2$ (12–19 cm^2/m^2)] was smaller than
the median high-RVEDAi [$20 \text{ cm}^2/\text{m}^2$ (16–23 cm^2/m^2)]. Nine patients (8%) had more
than moderate tricuspid regurgitation (TR). The TR velocity was 2.5 (2.2–2.9) m/s, and
30 patients (28%) were considered to have pulmonary hypertension from TR velocity
and inferior vena cava evaluation.

The CMR data are listed in Table 3. The median Qp/Qs ratio before transcatheter
closure was 2.4 (1.9–3.0) and after the closure was 1.1 (1.0–1.2). The median RVEDVi,
RVESVi, and RVEF were $137 \text{ mL}/\text{m}^2$ (109–172 mL/m^2), $69 \text{ mL}/\text{m}^2$ (54–85 mL/m^2), and
50% (45–53%), respectively. According to our definition, RV dilatation was observed
in 81 patients (76%).

248

249 *Agreement between TTE-RVEDAi and CMR-RVEDAi*

250

251 The Bland–Altman analysis showed that the difference between the iso-
RVEDAi and CMR-RVEDAi was $-3.9 \text{ cm}^2/\text{m}^2$, and the LOA was -1.0 to $8.8 \text{ cm}^2/\text{m}^2$.

252 The majority of patients (101, 94%) had smaller values than those measured using

253 CMR. By contrast, the difference between the high-RVEDAi and CMR-RVEDAi was

254 $0.3 \text{ cm}^2/\text{m}^2$, and the LOA was -3.7 to $4.3 \text{ cm}^2/\text{m}^2$. Only 42 patients (39%) had smaller

255 values than those measured using CMR (Figure 3).

256

257 *RV dilatation defined by the high-RVEDAi accuracy*

258 According to the CMR measurement, 81 patients had dilated RV and 26 had a

259 normal RV size. The relationship between high-RVEDAi and CMR-RVEDVi is shown

260 in Figure 4. The best cut-off value for detection by RV dilatation was $19.1 \text{ cm}^2/\text{m}^2$ 261 according to the receiver operating characteristic curve, with 96% specificity ~~and~~ 75%262 sensitivity, 98% positive predictive value, and 56% negative predictive value. Of the263 dilated RV group (n=81), 61 cases (75%) were classified as RV dilatation by high-264 RVEDAi. On the other hand, of the non-dilated RV group (n=26), 25 cases (96%)265 were classified as non-RV dilatation by high-RVEDAi. The predictive regression266 equation was $(\text{CMR-RVEDV} = 7.7 \times \text{RVEDA} - 21.4; \text{CMR-RVEDVi} = 7.5 \times \text{high-}$

RVEDAi-10.6). The correlation coefficient of high-RVEDA (TTE) and CMR-RVEDV
was $\rho = 0.83$.

Inter- and intra-observer variability

With regard to inter-observer variability, high-RVEDAi was shown to be superior to iso-RVEDAi. Intra-observer variability was excellent. The coefficient of variability and ICC data are shown in Table 4.

Discussion

In this study, we revealed that high-RVEDAi had greater agreement with CMR-RVEDAi than with iso-RVEDAi.

Importance of describing the entire RV

CMR can accurately measure RV volume with the availability of multiple sections. By contrast, the difficulty of depicting the entire RV using TTE underestimates the RV volume. In the 2019 ASE guidelines, an “RV focused view” is recommended, wherein “the apex of the LV is placed in the center and the basal diameter of the RV is maximized,” [25], and this view has an advantage over other views because of its good reproducibility [14]. However, in patients with dilated RV due to ASD, the entire RV often cannot be

書式を変更: スペルチェックと文章校正を行う 上付き下付き (なし)

書式を変更: スペルチェックと文章校正を行う 上付き下付き (なし)

visualized. In our study, it was ~~most~~most important to image the entire RV and clarify the RV wall. We ~~therefore~~ considered ~~that~~ the RV-focused view was important for measuring RV tracing. However, there were many cases in which it was difficult to visualize the entire RV using ~~the~~a typical RV-focused view. ~~Therefore~~Hence, we used a ~~four~~4-chamber view adjusted so that the RV was visualized to the maximum (RV-maximized view). This view maximized the entire RV, clearly identified the free wall of the RV, and avoided ~~the~~ ~~five~~-chambers, although the LV apex could not be centered in the scan sector due to the expansion of the RV. Because the RV-maximized view was a ~~four~~4-chamber view adjusted to measure the RV, this view was also used as an equivalent to the RV-focused view; this standard RV focused view might have not been appropriate for this study

Measuring the RV volume using 3D-TTE is also possible, but this approach has been reported to underestimate the value compared with CMR [2-7]. Therefore, to clarify the cause of underestimation, we examined the RVEDAi in the present study and scanned the RV as a whole, using the RV-focused view and the RV-maximized view.

RV tracing line

In CMR, RV tracing is undeviating, with the clear border of the RV cavity showing a high signal and the myocardial tissue showing a low signal. The description

書式を変更: スペルチェックと文章校正を行う 上付き下付き (なし)

305 of the RV free wall endocardial tracing method is unclear in the ASE guidelines [23-25].

書式を変更: スペルチェックと文章校正を行う 上付き下付き (なし)

306 Referring to the method used to demarcate the LV posterior wall in the parasternal long-
307 axis view, the isoechoic and high-echoic layers are considered as the myocardium and
308 pericardium, respectively.

309 However, in tracing the RV free wall, the current probe resolution partially
310 includes abundant trabeculations in the isoechoic area. Moreover, the boundary with the
311 echo-free area is blurred owing to the thin and flutter RV free wall. Therefore,
312 contouring the isoechoic layer in **TTE** can result in a smaller RVEDAi than that in
313 CMR.

314 By contrast, planimetry through the high-echoic border can avoid this
315 underestimation. The high-echoic area includes multiple structures, such as the RV
316 myocardium, epicardial adipose tissue, and pericardium. The thinness and adhesion of
317 all these structures disturb the visualization of the RV free wall as an isoechoic layer,
318 and affect the ability to distinguish from one another. However, the sufficient thinness
319 of these components disregards the limitation, and this method leads to an exact trace of
320 the RV free wall, with careful attention to artifacts for side lobes and multiple
321 reflections as myocardium. A **TTE** study with a contrast agent may **further** clarify
322 the border between the myocardium and pericardium.

The high-echoic line tracing method was shown to be superior to the isoechoic method in both consistency with CMR-RVEDAi and inter-observer reproducibility. The good reproducibility between examiners was likely due to the use of the high-echoic line as a mark. The high-echoic line tracing method is expected to be a useful method for future studies. Moreover, in the future, the high-echoic tracing method can be expected to improve the measurement accuracy of many inspections in clinical practice.

Contribution to 3D echocardiography

For the evaluation of RV volume, ASE guidelines have recommended the measurements of 3D-RV volumes [24]. However, the 3D-RV volume is smaller in TTE than in CMR [2-7]. Several reasons for this underestimation have been suggested. First, blurring of the RV endocardial border occurs more inside the RV tracing line [2]. Second, the RV anterior and outflow tract (RVOT) region disappears due to artifacts from the sternum [26, 27]. Indeed, the images of the anterior and RVOT regions are inadequate in 10 to 30% of cases, even when using the latest 3D systems [28].

The high-echoic line tracing method can make a clear trace line for the RV free wall. Muraru et al. [29] reported that the underestimation of the 3D-RV volume is improved by manually adjusting the trace line instead of performing automatic tracing. In contrast to 2D RV tracing, 3D-RV volume determination requires multiple traces to be

書式を変更: 上付き下付き(なし)

書式を変更: スペルチェックと文章校正を行う 上付き下付き(なし)

書式を変更: スペルチェックと文章校正を行う 上付き下付き(なし)

書式を変更: スペルチェックと文章校正を行う 上付き下付き(なし)

書式を変更: 上付き下付き(なし)

書式を変更: スペルチェックと文章校正を行う 上付き下付き(なし)

obtained via several cross sections (e.g., coronal view, short-axis view, etc.). The addition of the high-echoic line tracing method to these views can mitigate the underestimation of the 3D-RV volume and improve the inter-observer variability.

Clinical implication

The use of CMR is the gold standard for assessing right ventricular enlargement. However, there are cases in which CMR cannot be performed due to various reasons, such as non-MRI conditional pacemaker implantation and claustrophobia. In such cases, it is possible to evaluate right ventricular enlargement by using the RVEDAi of TTE. In addition, high-RVEDAi enables the improvement of inter-observer variability, as well as evaluation of RV enlargement. In our study, the high-RVEDAi was highly correlated with CMR-RVEDVi ($\rho = 0.83$), with ~~and~~ an optimal cutoff of $19.1 \text{ cm}^2/\text{m}^2$. The optimal cutoff was larger than the ASE guideline reference value of $13 \text{ cm}^2/\text{m}^2$. In our study, the cutoff of $19.1 \text{ cm}^2/\text{m}^2$ had high specificity and positive predictive value; therefore, ~~and so~~, it was possible to conclude that RV expansion was possible in almost all cases. This method has the same accuracy as RVEDAi of CMR, which is already considered to be very a useful technique. Contrast echo was very useful for clarifying the boundaries of RV and is considered a tool for better tracing. However, considering the time and effort, we thought it was not necessary to use it systematically.

~~We thought that contrast echo was possible to be very useful in cases with~~
~~extremely poor imaging of TTE. But~~However, contrast agent cannot be used clinically
 in Japan.

Study limitations

Several limitations associated with the present study warrant mentioning. First, this study was performed at a single center and included a small number of subjects. Therefore, a multicenter study should be conducted to verify our results. Second, we examined TTE-RVEDAi and CMR-RVEDAi only in patients with ASD. In these patients, the RV was dilated and ~~therefore only~~ patients with an enlarged RV were ~~only~~ assessed. ~~Thus, the~~ relationship between TTE-RVEDAi and CMR-RVEDAi in healthy subjects and patients with other heart diseases remains unclear. Third, the 3D-TTE RV volume was not performed on all patients because it was not available on all models. ~~Finally~~Fourth, high-RVEDAi was determined using a retrospective offline analysis. Fifth, ~~the study was associated with a there were high exclusion number, close to almost~~ 40% of ~~whole~~all the enrolled case. This high exclusion rate can be attributed to several parameters: ~~Some reasons were suggested; b~~Because this study was not prospective, a defined imaging manual ~~was not existed induring this study~~ was not available;

~~moreover. Also, we selected only highcases with high-quality images and with good~~
~~depiction of the trace line were selected.~~

Conclusions

High-RVEDAi showed more accurate agreement with CMR-RVEDAi than
with iso-RVEDAi. High-RVEDAi is expected to be the standard method for measuring
RV size using 2D-TTE.

Data Availability

The deidentified participant data will not be shared.

References

1. Stout KK, Daniels CJ, Aboulhosn JA, Bozkurt B, Broberg CS, Colman JM, et al. (2018) AHA/ACC guideline for the management of adults with congenital heart disease: A report of the American College of Cardiology/American Heart Association Task Force on Clinical Practice guidelines. *Circulation* 2019 139:e698–e800
2. Shimada YJ, Shiota M, Siegel RJ, Shiota T (2010) Accuracy of right ventricular volumes and function determined by three-dimensional echocardiography in comparison with magnetic resonance imaging: a meta-analysis study. *J Am Soc Echocardiogr* 23:943–953. <https://doi.org/10.1016/j.echo.2010.06.029>
3. Medvedofsky D, Addetia K, Patel AR, Sedlmeier A, Baumann R, Mor-Avi V, Lang RM (2015) Novel approach to three-dimensional echocardiographic quantification of right ventricular volumes and function from focused views. *J Am Soc Echocardiogr* 28:1222–1231. <https://doi.org/10.1016/j.echo.2015.06.013>
4. Ishizu T, Seo Y, Atsumi A, Tanaka YO, Yamamoto M, Machino-Ohtsuka T, et al (2017) Global and regional right ventricular function assessed by novel three-dimensional speckle-tracking echocardiography. *J Am Soc Echocardiogr* 30:1203–1213. <https://doi.org/10.1016/j.echo.2017.08.007>
5. Rajaram S, Swift AJ, Capener D, Elliot CA, Condliffe R, Davies C, et al (2012)

- 412 Comparison of the diagnostic utility of cardiac magnetic resonance imaging,
413 computed tomography, and echocardiography in assessment of suspected
414 pulmonary arterial hypertension in patients with connective tissue disease. *J*
415 *Rheumatol* 39:1265–1274. <https://doi.org/10.3899/jrheum.110987>
- 416 6. Greiner S, André F, Heimisch M, Aurich M, Steen H, Katus HA, Mereles D (2019)
417 A closer look at right ventricular 3D volume quantification by transthoracic
418 echocardiography and cardiac MRI. *Clin Radiol* 74:490.e7–490.e14.
419 <https://doi.org/10.1016/j.crad.2019.03.005>
- 420 7. Park JB, Lee SP, Lee JH, Yoon YE, Park EA, Kim HK, et al (2016) Quantification
421 of right ventricular volume and function using single-beat three-dimensional
422 echocardiography: A validation study with cardiac magnetic resonance. *J Am Soc*
423 *Echocardiogr* 29:392–401. <https://doi.org/10.1016/j.echo.2016.01.010>
- 424 8. Shiran H, Zamanian RT, McConnell MV, Liang DH, Dash R, Heidary S, et al
425 (2014) Relationship between echocardiographic and magnetic resonance derived
426 measures of right ventricular size and function in patients with pulmonary
427 hypertension. *J Am Soc Echocardiogr* 27:405–412.
428 <https://doi.org/10.1016/j.echo.2013.12.011>
- 429 9. Greutmann M, Tobler D, Biaggi P, Mah ML, Crean A, Oechslin EN, Silversides
430 CK (2010) Echocardiography for assessment of right ventricular volumes

- revisited: a cardiac magnetic resonance comparison study in adults with repaired tetralogy of Fallot. *J Am Soc Echocardiogr* 23:905–911. <https://doi.org/10.1016/j.echo.2010.06.013>
10. Schenk P, Globits S, Koller J, Brunner C, Artemiou O, Klepetko W, Burghuber OC (2000) Accuracy of echocardiographic right ventricular parameters in patients with different end-stage lung diseases prior to lung transplantation. *J Heart Lung Transplant* 19:145–154. [https://doi.org/10.1016/s1053-2498\(99\)00121-7](https://doi.org/10.1016/s1053-2498(99)00121-7)
11. Brown DW, McElhinney DB, Araoz PA, Zahn EM, Vincent JA, Cheatham JP, et al (2012) Reliability and accuracy of echocardiographic right heart evaluation in the U.S. Melody Valve Investigational Trial. *J Am Soc Echocardiogr* 25:383–392.e4. <https://doi.org/10.1016/j.echo.2011.12.022>
12. D’Anna C, Caputi A, Natali B, Leonardi B, Secinaro A, Rinelli G, et al (2018) Improving the role of echocardiography in studying the right ventricle of repaired tetralogy of Fallot patients: comparison with cardiac magnetic resonance. *Int J Cardiovasc Imaging* 34:399–406. <https://doi.org/10.1007/s10554-017-1249-1>
13. Alghamdi MH, Grosse-Wortmann L, Ahmad N, Mertens L, Friedberg MK (2012) Can simple echocardiographic measures reduce the number of cardiac magnetic resonance imaging studies to diagnose right ventricular enlargement in congenital heart disease? *J Am Soc Echocardiogr* 25:518–523.

<https://doi.org/10.1016/j.echo.2012.01.023>

14. Genovese D, Mor-Avi V, Palermo C, Muraru D, Volpato V, Kruse E, et al (2019)

Comparison between four-chamber and right ventricular-focused views for the quantitative evaluation of right ventricular size and function. *J Am Soc Echocardiogr* 32:484–494. <https://doi.org/10.1016/j.echo.2018.11.014>

15. Kou S, Caballero L, Dulgheru R, Voilliot D, De Sousa C, Kacharava G, et al

(2014) Echocardiographic reference ranges for normal cardiac chamber size: results from the NORRE study. *Eur Heart J Cardiovasc Imaging* 15:680–690. <https://doi.org/10.1093/ehjci/jet284>

16. Grünig E, Biskupek J, D'Andrea A, Ehlken N, Egenlauf B, Weidenhammer J, et al (2015) Reference ranges for and determinants of right ventricular area in healthy adults by two-dimensional echocardiography. *Respiration* 89:284–293.

<https://doi.org/10.1159/000371472>

17. Kort HW, Balzer DT, Johnson MC (2001) Resolution of right heart enlargement

after closure of secundum atrial septal defect with transcatheter technique. *J Am Coll Cardiol* 38:1528–1532. [https://doi.org/10.1016/S0735-1097\(01\)01547-9](https://doi.org/10.1016/S0735-1097(01)01547-9)

18. Veldtman GR, Razack V, Siu S, El-Hajj H, Walker F, Webb GD, et al (2001) Right

ventricular form and function after percutaneous atrial septal defect device closure. *J Am Coll Cardiol* 37:2108–2113. [https://doi.org/10.1016/S0735-1097\(01\)01305-](https://doi.org/10.1016/S0735-1097(01)01305-)

- 470 19. Yamasaki Y, Nagao M, Yamamura K, Yonezawa M, Matsuo Y, Kawanami S, et al
471 (2014) Quantitative assessment of right ventricular function and pulmonary
472 regurgitation in surgically repaired tetralogy of Fallot using 256-slice CT:
473 comparison with 3-tesla MRI. Eur Radiol 24:3289–3299.
474 <https://doi.org/10.1007/s00330-014-3344-1>
- 475 20. Alfakih K, Plein S, Bloomer T, Jones T, Ridgway J, Sivananthan M (2003)
476 Comparison of right ventricular volume measurements between axial and short
477 axis orientation using steady-state free precession magnetic resonance imaging. J
478 Magn Reson Imaging 18:25–32. <https://doi.org/10.1002/jmri.10329>
- 479 21. Pfluger HB, Maeder MT, LaGerche A, Taylor AJ (2010) One- and two-
480 dimensional estimation of right and left ventricular size and function-comparison
481 with cardiac magnetic resonance imaging volumetric analysis. Heart Lung Circ
482 19:541–548. <https://doi.org/10.1016/j.hlc.2010.03.003>
- 483 22. Rominger MB, Bachmann GF, Pabst W, Rau WS (1999) Right ventricular
484 volumes and ejection fraction with fast cine MR imaging in breath-hold technique:
485 applicability, normal values from 52 volunteers, and evaluation of 325 adult
486 cardiac patients. J Magn Reson Imaging 10:908–918.
487 [https://doi.org/10.1002/\(sici\)1522-2586\(199912\)10:6<908::aid-jmri2>3.0.co;2-2](https://doi.org/10.1002/(sici)1522-2586(199912)10:6<908::aid-jmri2>3.0.co;2-2)

- 488 23. Rudski LG, Lai WW, Afilalo J, Hua L, Handschumacher MD, Chandrasekaran K,
489 et al (2010) Guidelines for the echocardiographic assessment of the right heart in
490 adults: a report from the American Society of Echocardiography endorsed by the
491 European Association of Echocardiography, a registered branch of the European
492 Society of Cardiology, and the Canadian Society of Echocardiography. *J Am Soc*
493 *Echocardiogr* 23:685–713; quiz 786–688
- 494 24. Lang RM, Badano LP, Mor-Avi V, Afilalo J, Armstrong A, Ernande L, et al (2015)
495 Recommendations for cardiac chamber quantification by echocardiography in
496 adults: an update from the American Society of Echocardiography and the
497 European Association of Cardiovascular Imaging. *J Am Soc Echocardiogr* 28:1–
498 39.e14. <https://doi.org/10.1016/j.echo.2014.10.003>
- 499 25. Mitchell C, Rahko PS, Blauwet LA, Canaday B, Finstuen JA, Foster MC, et al
500 (2019) Guidelines for performing a comprehensive transthoracic
501 echocardiographic examination in adults: recommendations from the American
502 Society of Echocardiography. *J Am Soc Echocardiogr* 32:1–64.
503 <https://doi.org/10.1016/j.echo.2018.06.004>
- 504 26. Anwar AM, Soliman O, van den Bosch AE, McGhie JS, Geleijnse ML, ten Cate
505 FJ, Meijboom FJ (2007) Assessment of pulmonary valve and right ventricular
506 outflow tract with real-time three-dimensional echocardiography. *Int J Cardiovasc*

- 507 Imaging 23:167–175. <https://doi.org/10.1007/s10554-006-9142-3>
- 508 27. Ostenfeld E, Carlsson M, Shahgaldi K, Roijer A, Holm J (2012) Manual
509 correction of semi-automatic three-dimensional echocardiography is needed for
510 right ventricular assessment in adults; validation with cardiac magnetic resonance.
511 Cardiovasc Ultrasound 10:1. <https://doi.org/10.1186/1476-7120-10-1>
- 512 28. Seo Y, Ishizu T, Ieda M, Ohte N (2020) Right ventricular three-dimensional
513 echocardiography: the current status and future perspectives. J Echocardiogr
514 18:149–159. <https://doi.org/10.1007/s12574-020-00468-8>
- 515 29. Muraru D, Spadotto V, Cecchetto A, Romeo G, Aruta P, Ermacora D, et al (2016)
516 New speckle-tracking algorithm for right ventricular volume analysis from three-
517 dimensional echocardiographic data sets: validation with cardiac magnetic
518 resonance and comparison with the previous analysis tool. Eur Heart J Cardiovasc
519 Imaging 17:1279–1289. <https://doi.org/10.1093/ehjci/jev309>
- 520

Figure legends

Fig. 1 Apical four-chamber view of CMR. (a) Original image. (b) The CMR-RVEDA

tracing line is shown in dotted line.

Fig. 2 Apical four-chamber view of TTE. (a) Original image of the RV-maximized

view at the end-diastolic phase. (b) Isoechoic tracing. (c)

High-echoic tracing.

Small point, clarified part of the intermittently observed line. Dotted line, RVEDA

tracing line.

Fig. 3 Bland–Altman analysis of the relationship between the CMR-RVEDAi and

TTE-RVEDAi. (a) Iso-RVEDAi. (b) High-RVEDAi.

Fig. 4 Relationship between the high-RVEDAi and CMR-RVEDVi. The horizontal

broken line represents the cut-off value of RV dilatation (107.5 mL/m^2). The vertical

broken line represents the best cut-off value of the high-RVEDAi ($19.1 \text{ cm}^2/\text{m}^2$). Linear

regression is shown in red solid line; non-linear regression (quadratic curve) is shown in

blue solid line.

Table 1. Patient characteristics

	n=107
Age, years	59 (44-67)
Male, n	28 (26)
Height, cm	158 (153-164)
Weight, kg	55 (48-62)
BSA, m ²	1.53 (1.43-1.67)
HR, beats/min	65 (60-72)
SpO ₂ (<i>n</i> =98), %	98 (97-99)
SBP (<i>n</i> =59), mmHg	116 (108-128)
DBP (<i>n</i> =59), mmHg	70 (60-76)
NYHA (<i>n</i> =101)	
I	72 (71)
II	29 (29)
III	0 (0)
IV	0 (0)
12ECG	
Sinus rhythm	103 (96)
AF	4 (4)

Data are expressed as number (percentage) or median (interquartile range).

BSA, body surface area; HR, heart rate; SBP, systolic blood pressure; DBP, diastolic blood pressure; NYHA, New York Heart Association; AF, atrial fibrillation.

Table 2. Echocardiographic characteristics

	n=107
LVDd, mm	42 (38-47)
LVDs, mm	25 (23-28)
LVEDV, mL	71 (60-90)
LVESV, mL	24 (20-31)
LVEDVi, mL/m ²	46 (39-54)
LVESVi, mL/m ²	16 (12-20)
LVEF, %	65 (60-69)
LAD, mm	36 (32-42)
LAVi, mL/m ²	34 (27-43)
RA area, cm ²	18 (15-23)
isoechoic line tracing RVEDAi, cm ² /m ²	15 (12-19)
high-echoic line tracing RVEDAi, cm ² /m ²	20 (16-23)
TR velocity, m/s (<i>n</i> =105)	2.5 (2.2-2.9)
More than moderate TR, n	9 (8)
IVCD, mm	15 (13-18)
Estimated RAP, mmHg	3 (3-3)
TAPSE, mm (<i>n</i> =105)	24 (21-28)

Data are expressed as number (percentage) or median (interquartile range).

LVDd, left ventricular end-diastolic diameter; LVDs, left ventricular end-systolic diameter; LVEDV, left ventricular end-diastolic volume; LVESV, left ventricular end-systolic volume; LVEDVi, left ventricular end-diastolic volume index; LVESVi, left ventricular end-systolic volume index; LVEF, left ventricular ejection fraction; LAD, left atrial diameter; LAVi, left atrial volume index; RA, right atrial; RVEDAi, right ventricular end-diastolic area index; TR, tricuspid regurgitation; IVCD, inferior vena cava diameter; RAP, right atrial pressure; TAPSE, tricuspid annular plane systolic excursion; TDI, tissue Doppler imaging;

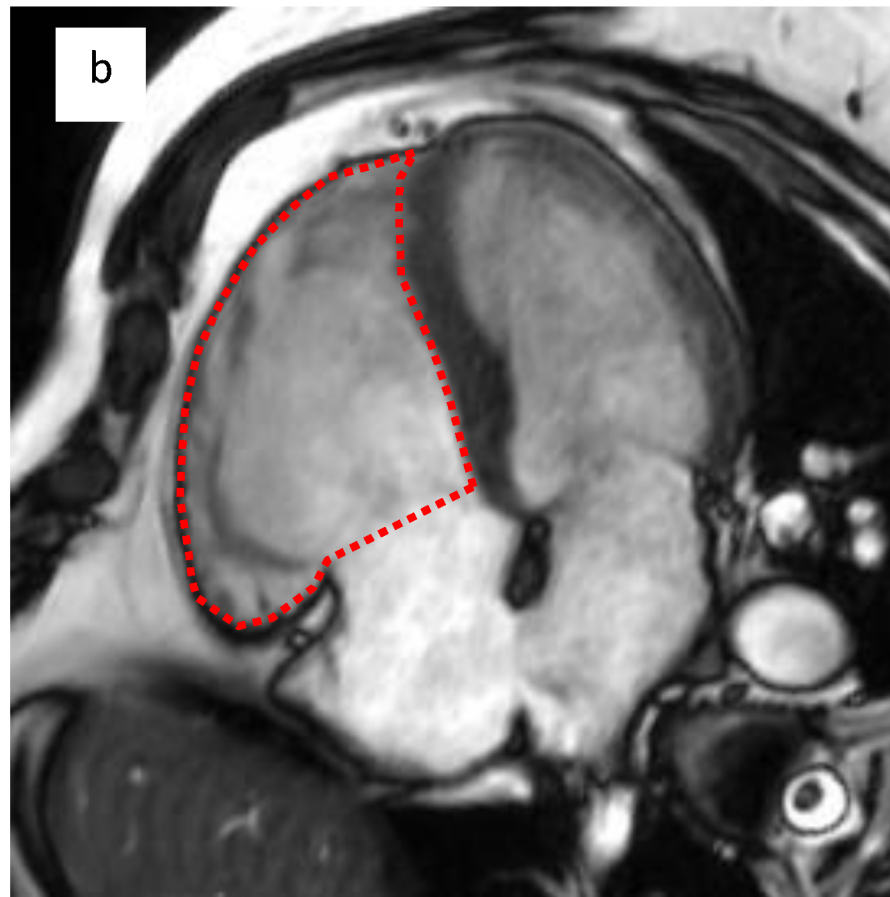
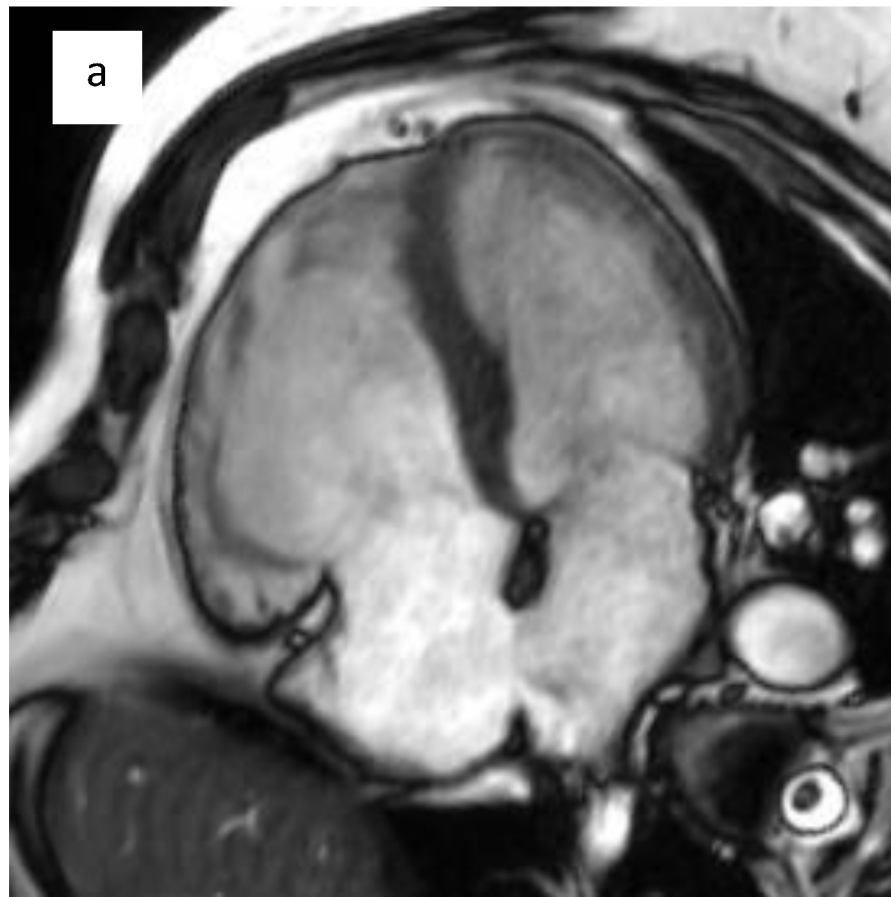
Table 3. CMR characteristics

variable	value
RVEDA _i , cm ² /m ²	20 (16-23)
RVEDV _i , mL/m ²	137 (109-172)
RVESV _i , mL/m ²	69 (54-85)
RVEF, %	50 (45-53)
LVEDV _i , mL/m ²	70 (54-85)
LVESV _i , mL/m ²	32 (25-38)
LVEF, %	56 (50-62)
HR, beats/min	62 (56-69)
Q _p , L/min	5.7 (4.4-8.0)
Q _s , L/min	3.7 (3.0-4.3)
Q _p /Q _s ratio	
Before transcatheter closure of ASD	2.4 (1.9-3.0)
After transcatheter closure of ASD	1.1 (1.0-1.2)

Data are expressed as number (percentage) or median (interquartile range).

RVEDV_i, right ventricular end-diastolic volume index; RVESV_i, right ventricular end-systolic volume index; RVEF, right ventricular ejection fraction; LVEDV_i, left ventricular end-diastolic volume index; LVESV_i, left ventricular end-systolic volume index; LVEF, left ventricular ejection fraction;

HR, heart rate; Q_p , pulmonary blood flow; Q_s , systemic blood flow;



a

v

5

10

b

Isoechoic
line tracing

v

5

10

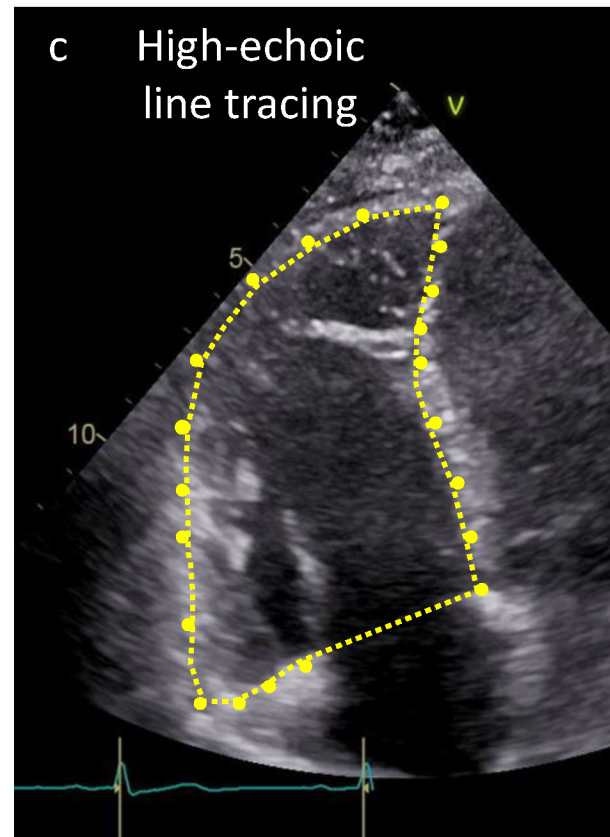
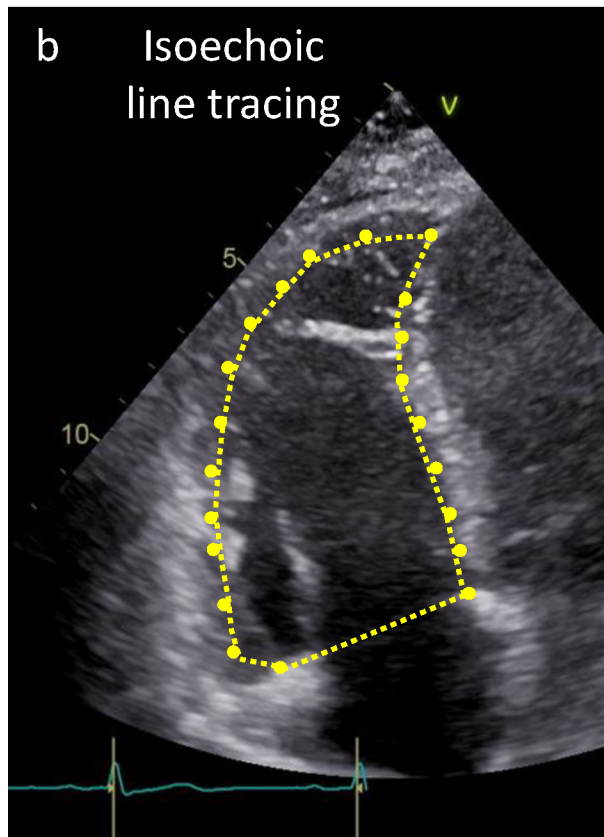
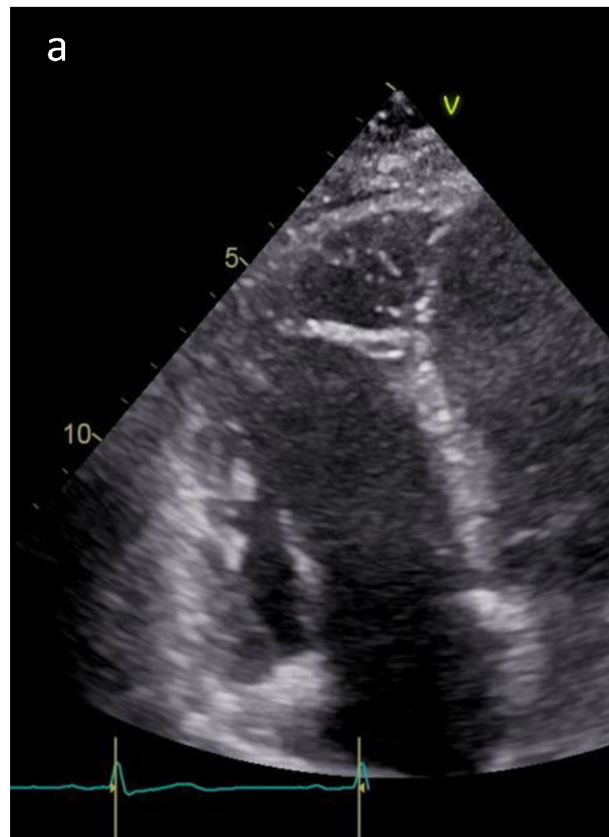
c

High-echoic
line tracing

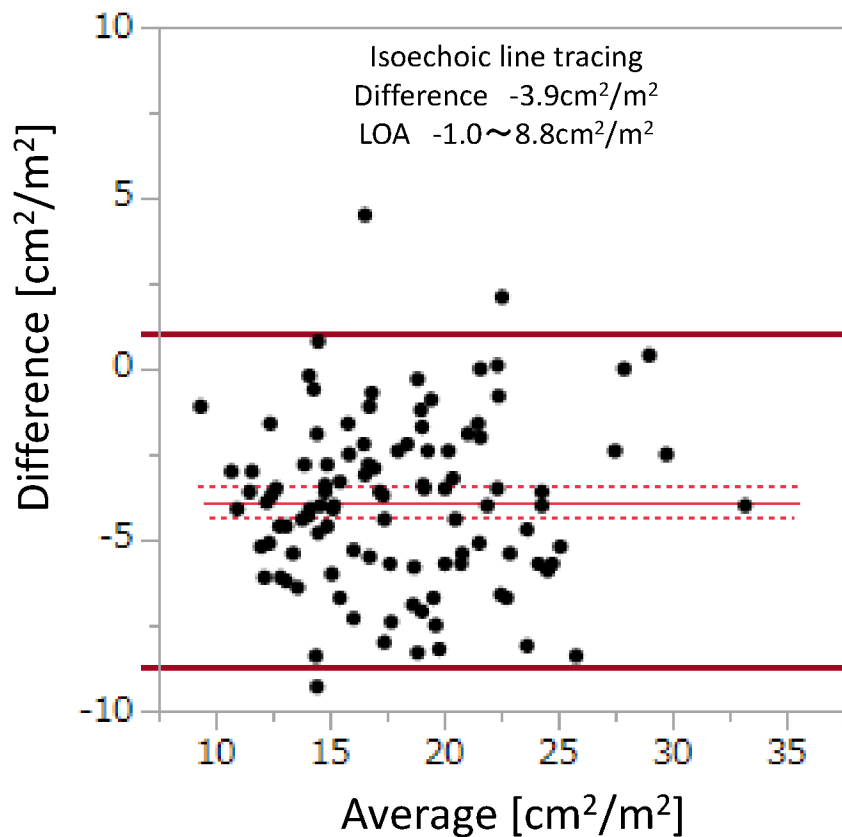
v

5

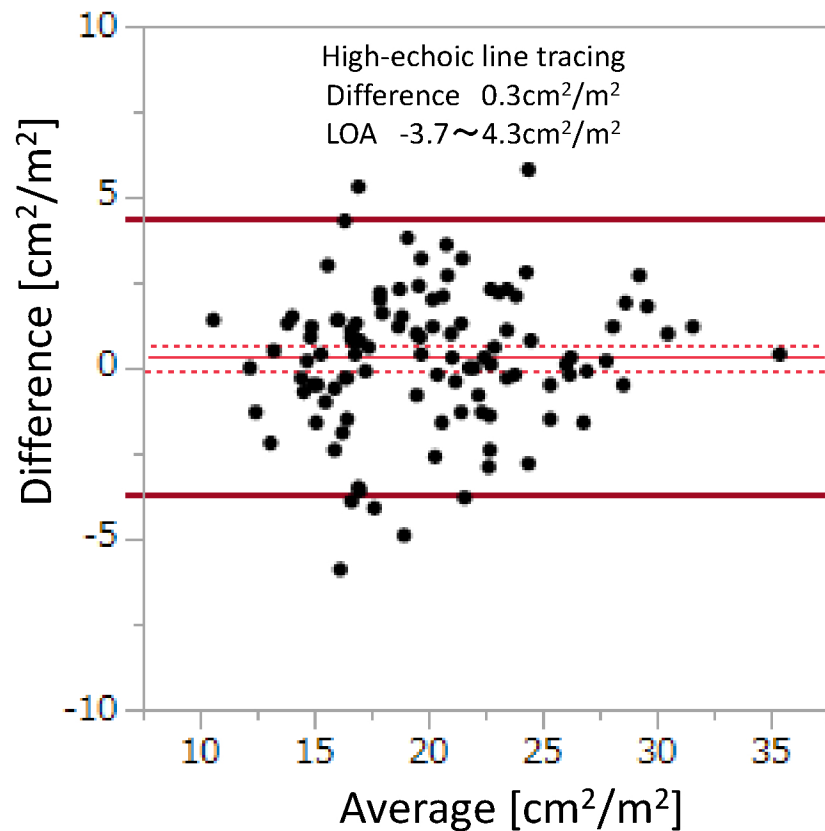
10



a



b



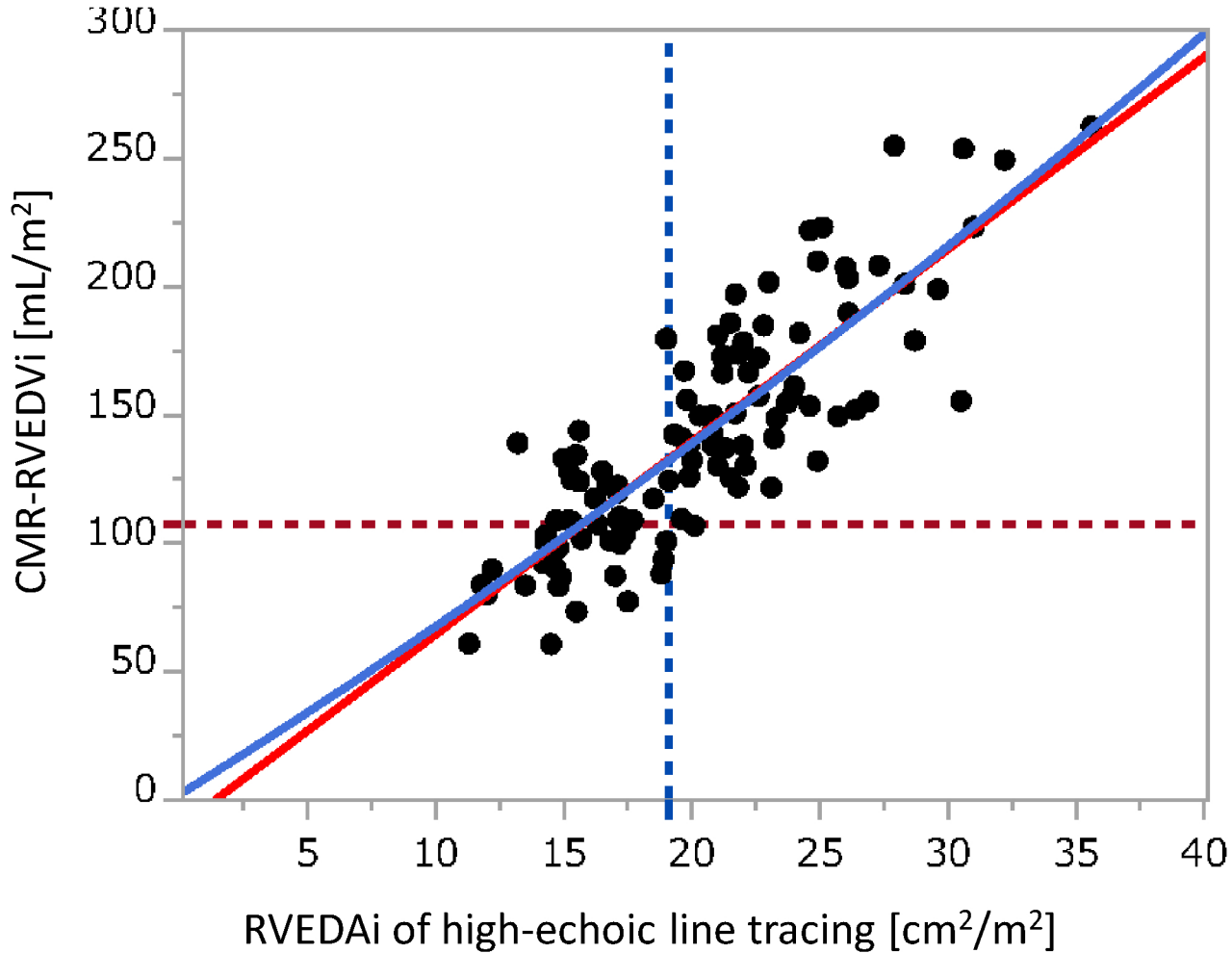


Table 4. Inter- and intra-observer variability

	Inter-observer		Intra-observer	
	variability		variability	
	CoV (%)	ICC	CoV (%)	ICC
Isoechoic line tracing	10.2 ± 3.6	0.91	-	-
High-echoic line tracing	6.8 ± 2.6	0.95	3.9 ± 3.0	0.96

CoV are expressed as mean ± SD. ICC are expressed as percentage.

CoV, coefficient of variation; ICC, intraclass correlation coefficient